6902 *Macromolecules* **2009**, *42*, 6902–6916
DOI: 10.1021/ma9013077

Macromolecules
ARTICLE

Intrachain Electron and Energy Transfers in Metal Diynes and Polyynes of Group 10−11 Transition Elements Containing Various Carbazole and Fluorene Hybrids

Shawkat M. Aly,[†] Cheuk-Lam Ho,[‡] Wai-Yeung Wong,*[,‡] Daniel Fortin,[†] and Pierre D. Harvey*[,†]

[†]*Département de chimie, Université de Sherbrooke, 2550 Boul. Université, Sherbrooke, PQ, J1K 2R1 Canada, and* [‡]*Department of Chemistry and Centre for Advanced Luminescence Materials, Hong Kong Baptist University, Waterloo Road, Kowloon Tong, Hong Kong, P.R. China*

Received June 17, 2009

ABSTRACT: A series of soluble and thermally stable group 10 platinum(II) polyyne polymers of the type $[-C\equiv C-Pt(PBu_3)_2-C\equiv C-\mathbf{X}-]_n$ along with their corresponding dinuclear model compounds $[Ph-Pt(PEt_3)_2-C\equiv C]_2-\mathbf{X}-$ and $[Ph_3P-Au-C\equiv C]_2-\mathbf{X}-$ where **X** = **F**, **Cz**′, **Cz**, **Cz**−**F**, (**Cz**)$_2$, (**Cz**)$_3$ and **Cz**−**F**−**Cz**; **F** = 2,7-fluorene, **Cz**′ = 2,7-carbazole, **Cz** = 3,6-carbazole, were prepared and characterized. The electronic spectra (absorption, excitation, emission and ns transient absorption spectra) and the photophysical properties of these metalated compounds in 2MeTHF at 298 and 77 K are reported. These findings are correlated to the computational data obtained by density functional theory (DFT). Evidence for intramolecular singlet electron and triplet energy transfers from the **Cz** chromophore to the **F** moiety is provided and discussed in detail for those with organic spacers consisting of the carbazole−fluorene hybrids. The rate for electron transfer is very rapid ($k_{et} > 4 \times 10^{11}$ s^{-1} at 298 K) whereas that for triplet−triplet energy transfer is much slower ($k_{ET} \sim$ ca. 10^3 s^{-1} time scale). The k_{ET} values for the digold dyads are lower than that found for the diplatinum analogues, which are slower than the corresponding platinum-containing polymers. The observed increase in k_{ET} for the dinuclear systems is explained by the triplet excited state population of the diplatinum species as compared to the digold congener, and for the polymers, the larger rates (twice as fast) are due to the presence of two fluorene chromophores flanking the carbazole-containing unit, hence providing two pathways to relaxation.

Introduction

The search for new metal−organic molecular functional materials with optoelectronic capabilities continues to attract much current research attention.[1] Among these, conjugated organometallic poly(aryleneethynylenes)s and their model oligomers,[2] have extensively been studied. Exhaustive studies of these materials over the past decade have made it possible to clarify some fundamental issues about the nature of the singlet excited states,[3] yet still relatively little is known about detailed photophysics that can address the electronic communication in the conjugated backbones. Much of the recent work has shown that triplet states play an important role in optical and electrical processes within conjugated polymers with direct implications for their technological exploitation.[4] While the ultimate efficiency of organic light-emitting diodes (OLEDs) is typically controlled by the fraction of triplet states generated or harvested,[5] a thorough understanding and examination of triplet photophysics is essential in conjugated polymers. This can be achieved by the incorporation of platinum atom within the conjugated backbone in which strong spin−orbit coupling associated with such heavy metal renders the spin-forbidden triplet, T_1, emission partially allowed and experimentally accessible. Similar research work has been extended to their closest neighbors, viz, gold(I)[6] and mercury(II)[7] with fruitful results.

While studies on mixed-aryl carbazole−fluorene-based organic dyads, polyads, oligomers, polymers and dendrimers[8−11] constitute an important research topic in the field of optoelectronics including photovoltaic cells and both OLEDs and polymer light-emitting diodes (PLEDs), work on the corresponding organometallic polymers is still in its infancy, especially from a photophysical viewpoint.[1f,2,12] These carbazole (**Cz**) and fluorene (**F**) aromatics are prone for singlet electron transfer[13] and T_1 energy transfer,[13] including the case in the **Cz**−**F** dyad,[14] hence featuring important properties toward practical optoelectronic applications. Recently, the use of heavy metal-containing bisethynyl linkers to form conjugated carbazole- and fluorene-based poly(aryleneethynylene)s of platinum, gold, and mercury was made and the emission spectroscopy and photophysics were extensively investigated.[6,7] The key feature is that the incorporation of a heavy metal in the backbone of the polymers can indeed facilitate intersystem crossing, hence strongly populating the T_1 excited states. The enhancement in T_1 state population leads on one hand to the potential application of white light emission in OLEDs and PLEDs, but also on a fundamental standpoint, to other channels of photoinduced electronic communication such as the T_1 energy transfer along the molecular main chain on (donor−acceptor)-containing organometallic polymers. In this connection, the resulting optoelectronic properties can be controlled and optimized through structural modifications of the donor−acceptor motifs.[15]

In this context, we have recently investigated some metal oligomers and polymers of the type $[Ph-PtL'_2-C\equiv C-\mathbf{Cz}]_2-\mathbf{X}-$ and $[-\mathbf{Cz}-C\equiv C-PtL_2-C\equiv C-\mathbf{Cz}-\mathbf{X}-]_n$, where **Cz** = 3,6-carbazole, **X** = nothing, **Cz** or **F** (2,7-fluorene), L = PBu_3 and L′ = PEt_3.[15] Carbazole trimers linked at 3,6- and 2,7-positions have

*Corresponding authors. E-mail: (W.-Y.W.) rwywong@hkbu.edu.hk; (P.D.H.) Pierre.Harvey@USherbrooke.ca.

 Published on Web 08/20/2009

Chart 1. Chemical Structures of Group 10−11 Metalated Compounds in This Work

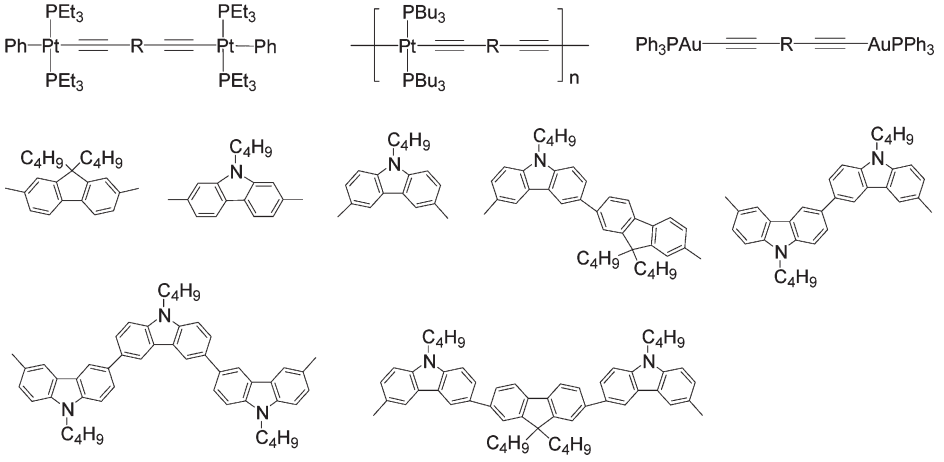

been studied before.[15] The comparison between these two showed that they have two different situations. While in the 3,6-linked carbazole trimers there is no conjugation over large distance and the triplet wave function is limited to one carbazole unit, the 2,7-linked species showed it to be a highly conjugated molecule.[15,16] Here we report the characterization of the photophysical properties of 2,7-dimetalated carbazole and 2,7-dimetalated fluorene complexes and their polymers in order to study the effect of polymerization on the photophysical properties. The 2,7-dimetalated carbazole is studied for comparison reasons with that for the 3,6-carbazole. Also, the studied compounds are either Au or Pt derivatives to account for the effect of the metal on the corresponding photophysical properties. Another purpose of this study is aimed at investigating the photophysical properties of the carbazole−fluorene dyads and the carbazole−fluorene−carbazole triads and the change in their photophysical properties in comparison with the fluorene and carbazole analogues (Chart 1). The electronic spectra and the photophysics of these metalated materials in 2MeTHF at 298 and 77 K are presented. A discussion on the evidence for S_1 and T_1 energy transfers from the **Cz** chromophore to the **F** moiety is made. Based on the results, the rate for electron transfer is fast ($>4 \times 10^{11}$ s^{-1} at 298 K) whereas that for T_1 energy transfer is much slower ($\sim 10^3$ s^{-1} time scale). The effect of metal groups (gold versus platinum) on the T_1 energy transfer rate was also examined. This work addresses the electronic communication in the backbone of a conjugated organometallic polymer.

Experimental Section

General. All reactions were carried out under a nitrogen atmosphere with the use of standard Schlenk techniques, but no special precautions were taken to exclude oxygen during workup. Solvents were predried and distilled from appropriate drying agents. All reagents and chemicals, unless otherwise stated, were purchased from commercial sources and used without further purification. Preparative TLC was performed on 0.7 mm silica plates (Merck Kieselgel 60 GF_{254}) prepared in our laboratory. The compounds *trans*-[$PtCl(Ph)(PEt_3)_2$],[17] *trans*-[$PtCl_2(PBu_3)_2$],[18] **L3**, **M3**, **P3**,[19] **L5**−**L7**, **M5**−**M7**, and **P5**−**P7**[15] were prepared by literature methods. Infrared spectra were recorded as CH_2Cl_2 solutions using a Perkin-Elmer Paragon 1000 PC or Nicolet Magna 550 Series II FTIR spectrometer, using CaF_2 cells with a 0.5 mm path length. NMR spectra were measured in appropriate solvents on a Jeol EX270 or a Varian Inova 400 MHz FT-NMR spectrometer, with ^1H and ^{13}C NMR chemical shifts quoted relative to $SiMe_4$ and ^{31}P chemical shifts relative to an 85% H_3PO_4 external standard. Fast atom bombardment (FAB) mass spectra were recorded on a Finnigan MAT SSQ710 mass spectrometer. The molecular weights of the polymers were determined by GPC (HP 1050 series HPLC with visible wavelength and fluorescent detectors) using polystyrene standards and thermal analyses were performed with a Perkin-Elmer DTA-7 thermal analyzer. The photophysical measurements were carried out in 2MeTHF, which was distilled over calcium hydride under argon. UV−visible spectra were recorded on a Varian Cary 300 spectrophotometer. The emission spectra were obtained using a double monochromator Fluorolog 2 instrument from Spex. The emission lifetimes were measured on a TimeMaster Model TM-3/2003 apparatus from PTI. The source was nitrogen laser with high-resolution dye laser (fwhm $\sim$ 1400 ps), and the fluorescence lifetimes were obtained from deconvolution or distribution lifetimes analysis. The uncertainties were about 50−100 ps (ps = picosecond). The time-resolved spectra were performed on a PTI LS-100 using a 1 μs tungsten-flash lamp (fwhm $\sim$ 1 μs). The flash photolysis spectra and the transient lifetimes were measured with a Luzchem spectrometer using the 355 nm line of a YAG laser from Continuum (Serulite), and the 530 nm line from OPO module pump by the same laser (fwhm = 13 ns).

Quantum Yield Measurements. Measurements were performed in 2MeTHF at 298 and 77 K. All of the samples were prepared under inert atmosphere (in a glovebox, $P_{O_2} < 50$ ppm). For both temperatures, the sample and standard concentrations were adjusted to obtain an absorbance of 0.05 or less. This absorbance was adjusted to be the same as much as possible for the standard and the sample for a measurement. Each absorbance value was measured ten times for better accuracy in the measurements of the quantum yields. The reference used for quantum yield was 9,10-diphenylanthracene ($\Phi_F = 1.0$).[20]

Theoretical Computations. Calculations were performed on an Intel Xeon 3.40 GHz PC with the Gaussian 03 revision C.02 and Gausview 3.0 software package. The hybrid B3LYP exchange-correlation function has been used.[21] LANL2DZ pseudopotentials and basis sets were used for platinum, 3-21G* pseudopotentials for phosphorus, and 3-21G* basis sets for all atoms[22] except for platinum. The platinum structure file was optimized before the TDDFT calculation. Only the relevant (stronger oscillator strength and wave function coefficients) molecular orbitals are shown.

Syntheses. The syntheses of new diethynyl ligands and metal diynes and polyynes are given in the Supporting Information.

Results and Discussion

Synthesis. The synthetic routes leading to the target molecules **L1**−**L7** are outlined in Schemes 1 and 2. The synthesis of the key intermediate to the dibromide precursor of **L4** was first prepared by alkylation of carbazole with 1-bromobutane. Subsequently, 9-butylcarbazole was brominated with one equivalent of *N*-bromosuccinimide (NBS) to afford

3-bromo-9-butylcarbazole. This compound was converted to its 9-butylcarbazole-3-boronic acid and coupled with 2-bromo-7-iodo-9,9-dibutylfluorene.[23] Effort was spent in order to couple it with 2-bromo-9,9-dibutylfluorene. However, bromination of the resulting product by bromine leads to the multisubstitution of carbazole by bromides. In parallel, no substitution on fluorene was observed when NBS was used. Therefore, we used 9-butylcarbazole-3-boronic acid to couple to 2-bromo-7-iodo-9,9-dibutylfluorene.[23] In this case, the reaction was heated up to only 50 °C in order to leave the bromo site unreacted. All of the halogenated precursors were then reacted with $Me_3SiC{\equiv}CH$ via the Sonogashira coupling sequence,[24] followed by the proto-desilylation reaction with K_2CO_3 in MeOH at room temperature to afford the diethynyl organic precursors $\mathbf{L_1}-\mathbf{L_7}$. Scheme 3 shows the chemical structure and the synthetic strategies used to prepare, via the classical dehydrohalogenation methods, polymers **P1**−**P7** and their model complexes (**M1**−**M7** and **A1**−**A7**).[2,25,26]

Chemical Characterization. All of the new metal complexes and polymers are air-stable and generally exhibit good solubility in chlorocarbons such as CH_2Cl_2 and $CHCl_3$. GPC analysis was used to estimate the molecular weight of each polymer (see Experimental Section). However, the data should be viewed with caution in view of the difficulties associated with utilizing GPC for rigid-rod polymers which would have appreciable differences in the hydrodynamic behavior from those for flexible polystyrene polymers. Hence, we would anticipate certain systematic errors in the GPC measurements.[12d] However, the lack of discernible resonances that could be attributed to end groups in the NMR spectra provides support for the view that there is a high degree of polymerization in most of these polymers. The thermal properties of new polymers were examined by thermal gravimetric analysis (TGA) under nitrogen. Analysis of the TGA trace (heating rate of 20 °C min^{-1}) for the polymers shows that they have high onset decomposition temperatures ($T_{dec} \sim 283-352$ °C), indicative of their excellent thermal stability. Their degradation patterns are quite similar and we observe sharp weight losses of 27 to 42%, corresponding to the loss of PBu_3 and butyl groups from the polymers. The onset temperatures for **P1** and **P4**−**P7** (348−352 °C) are comparable to each other but are higher than those in **P2** (283 °C) and **P3** (315 °C) as well as related polymers *trans*-$[-Pt(PBu_3)_2C{\equiv}CRC{\equiv}C-]_n$ (R = phenylene, thienylene, pyridyl, 278−320 °C) and *trans*-$[-Pt(PBu_3)_2C{\equiv}C(p\text{-}C_6H_4)_2C{\equiv}C-]_n$ (296 °C).[2a]

Scheme 1. Synthetic Routes to the 3-Bromo-6-(2-bromo-9,9-dibutylfluoren-7-yl)-9-butylcarbazole

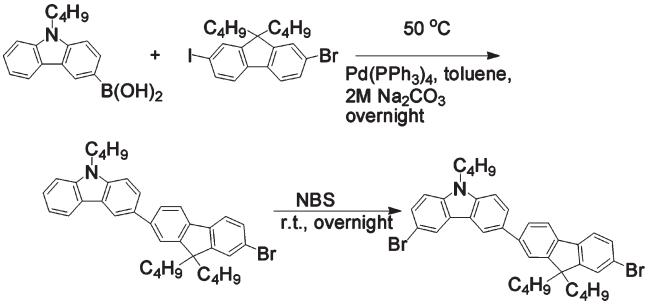

The good solubility for these new compounds renders them amenable to spectroscopic studies. Systematic characterization of these new compounds was achieved by analytical and spectroscopic methods (see Supporting Information). The IR, NMR (^1H, ^{13}C and ^{31}P) and mass spectral data are in accordance with their chemical structures. The solution IR spectra of these metal complexes display a single sharp $\nu(C{\equiv}C)$ absorption band, revealing a *trans*-configuration of the ethynylene ligands around the metal center for the platinum dimeric molecules. The absence of the C≡C−H stretching mode at around 3300 cm^{-1} of each compound indicates the formation of M−C≡C bond. The NMR spectral data supported the conclusion that these compounds have well-defined and symmetrical structures. The ^{31}P NMR spectra of the platinum(II) complexes exhibit a single resonance with a pair of ^{195}Pt satellites that confirms the *trans*-arrangement of the phosphine ligands around platinum. The $^1J_{P-Pt}$ values in the Pt diynes (ca. 2629−2643 Hz) are typical of those found for related *trans*-PtP_2 systems. Notably, two distinct ^{13}C NMR signals for the α- and β-acetylenic carbon atoms in these complexes are observed and the α-acetylide chemical shifts are shifted downfield with respect to the free ligands. The aromatic region of their ^{13}C NMR spectra also gives more precise information about the regiochemical structure of the main-chain skeleton and reveals a high degree of structural regularity in the polymers. The formulas of discrete molecules were also established by the observation of intense molecular ion peaks in the positive FAB mass spectra.

Optical Absorption and Photoluminescence Spectroscopy. Table 1 presents the peak positions in absorption and emission spectra of all investigated molecules.

Scheme 2. Syntheses of the Diethynyl Precursors

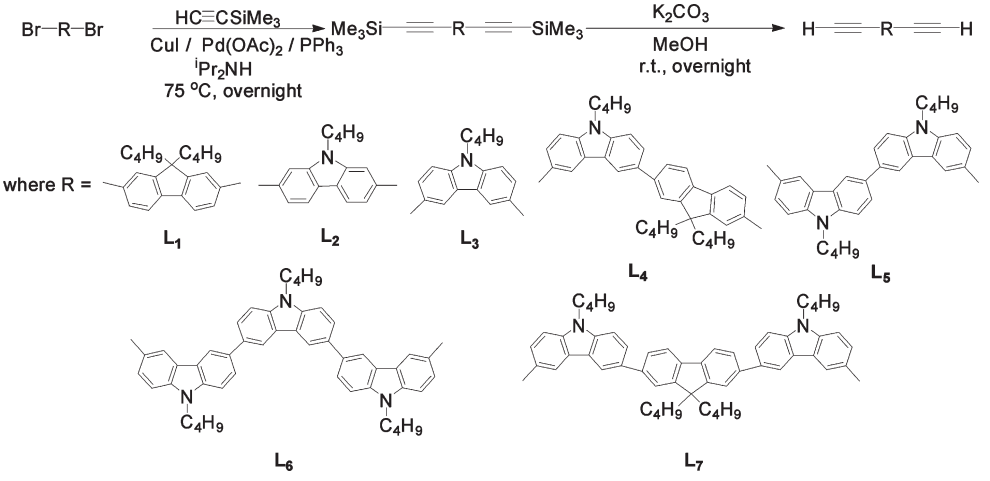

Scheme 3. Syntheses of the Investigated Compounds and Polymers

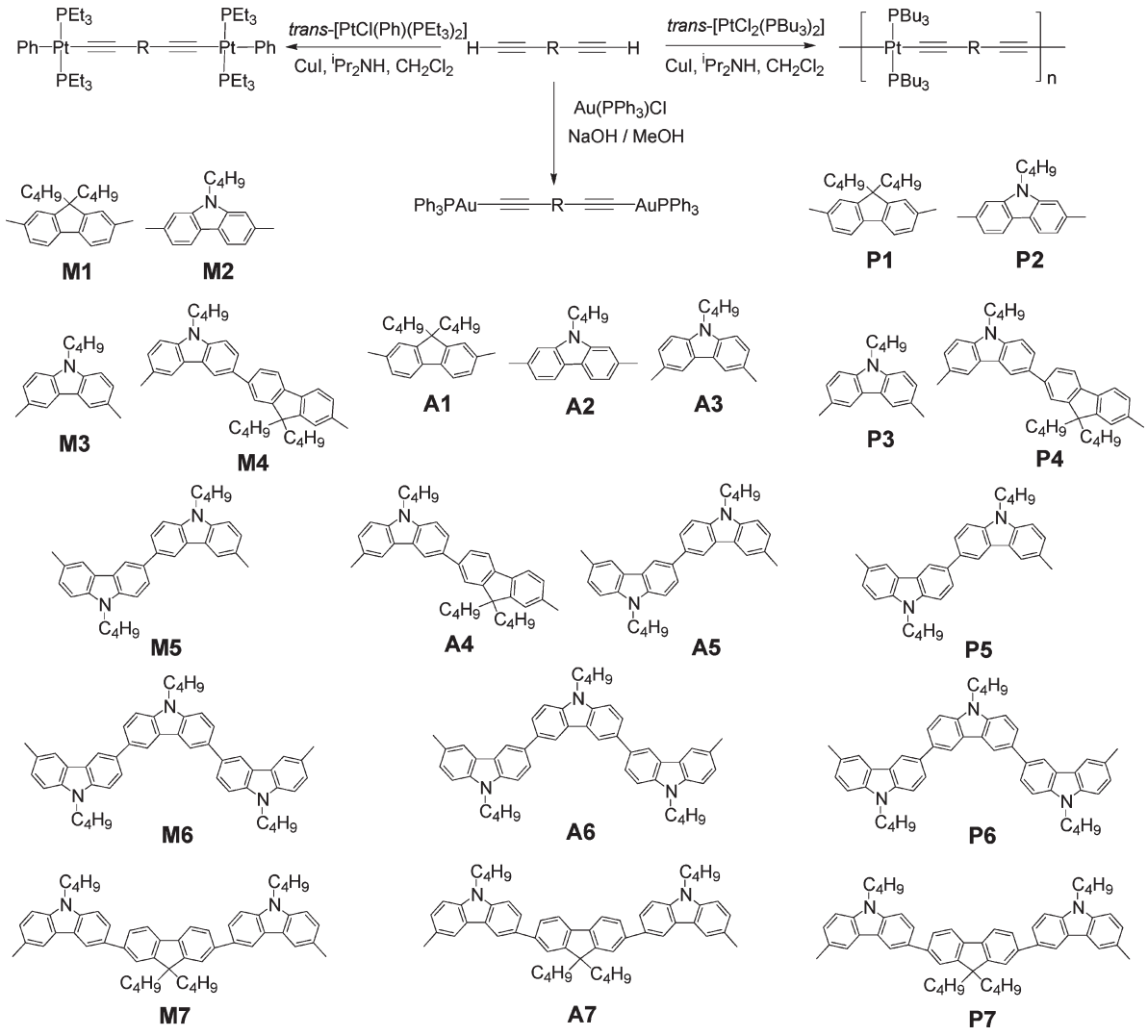

Absorption. The observed absorption for all the studied compounds showing a similar structured absorption spectrum suggests that the lowest energy bands can be assigned to ligand-centered $\pi-\pi^*$ transitions with a possibly mixed contribution from some admixture of metal orbitals for the metal-containing compounds.[2c,27] A clear red shift is observed in absorption wavelength when we compare the ligand with the metalated analogue which can be attributed to π-conjugation of the ligands into and through the metal center.[2]

Emission. There are two different types of compounds to address: first, the dimetalated fluorene and carbazole species and their corresponding polymers, second, the mixed carbazole−fluorene compounds and their dimetalated analogues as dyads and triads. The photoluminescence (PL) properties of **M5**−**M7** and **P5**−**P7** have been reported recently.[15]

Emission of the Dimetalated Compounds. *Emission of 2,7-Fluorene System.* The emission spectra measured for 2,7-diethynyl-9,9-dibutylfluorene and its corresponding platinum(II) and gold(I) derivatives as well as the platinum-(II) polymers in 2MeTHF at 77 K are given in Figure 1 and the 298 K spectra are shown in Supporting Information (see Figure S1). The observed emission at 77 K for the 2,7-fluorene exhibits a fluorescence band with some vibronic structure over the range of 330−400 nm and the phosphorescence is not observed. On the other hand, the PL spectra for the metal-containing analogues showed an enhancement of the phosphorescence bands over the range between 550−750 nm. The increase of the phosphorescence for the metal-containing compounds is due to the mixing of S_1 and T_1 states induced by the spin−orbit coupling of the heavy atom and the increased rate of intersystem crossing.[28] The spectrum for the corresponding polymer of the platinum analogue **P1** was recorded for comparison purpose with its monomer analogue, **M1**, and to study the effect of polymerization on the photophysical properties. The spectra for the polymer are characterized by fluorescence emission over the range of 400−440 and strong phosphorescence in the range of 550−750 nm.

The fluorescence bands were observed at 388 and 411 nm for diplatinum 2,7-fluorene (**M1**), while these peaks are red-shifted (∼30 nm) to 416 and 443 nm for its corresponding polymer (**P1**). A similar but smaller shift (∼7 nm) was also observed for the phosphorescence bands from 545 nm for the λ_{0-0} phosphorescence emission in **M1** to 552 nm in polymer **P1**. These red-shifts can be attributed to the increased conjugation associated with the polymerization.

The emission spectra of $\mathbf{L_1}$ and **A1** in 2MeTHF at 298 K are given in the Supporting Information (Figure S1). Both of the ligand $\mathbf{L_1}$ and its corresponding digold complex **A1** showed only the structured fluorescence band spreading over the range 330−400 and 400−500 nm, respectively. On

Table 1. UV−Vis Absorption and Emission Data at 298 and 77 K in 2MeTHF

	absorption λ (nm) 298 K	PL λ (nm) 298 K	PL λ (nm) 77 K
$\mathbf{L_1}$	292, 303, 316, 330	333, 349	
A1	372	402, 425	417, 442, 469, 569,[b] 662
M1	358, 374	388, 404, 541,[b] 597	388, 411, 545,[b] 587, 598, 618, 647, 663
P1	310, 392	409, 431, 550,[b] 593	416, 443, 552,[b] 595, 606, 626, 654, 672
$\mathbf{L_2}$	260, 314, 326, 356, 374	381, 401	
A2	250, 348, 369	382, 399, 509,[b] 555	379, 400, 425, 491, 501,[b] 523, 533, 546, 585, 602
M2	236, 264, 358, 376	385, 402, 522,[b] 565	384, 404, 513,[b] 560
P2	264, 390	408, 428, 527,[b] 567	414, 436, 524,[b] 572
$\mathbf{L_3}$	297, 306, 330, 345, 361	365, 385	
A3	264, 290, 316	382, 400, 437,[b] 468, 481	381, 403, 433,[b] 459, 466, 477
M3	288, 300, 334, 345	397, 420	450,[b] 481, 496
P3	304, 332	408, 430	402, 426, 460,[b] 483, 497, 510
$\mathbf{L_4}$	254, 286, 314, 340	384, 398	
A4	318, 354	397, 417	397, 419, 446, 532,[b] 580
M4	328, 364	400, 418, 544,[b] 584	397, 419, 446, 532,[b] 580
P4	272, 288, 374	400, 422, 545,[b] 587	407, 434, 543,[b] 591
A5	248, 318	420, 437,[b] 472	386, 408, 437, 451,[b] 482
A6	250, 318	420	397, 416, 438,[b] 453, 468, 483
A7	244, 316, 355	397, 416	397, 419, 438, 445, 472, 529,[b] 570, 610
M5[a]	258, 290, 310, 325	350, 415	395, 415, 446,[b] 478, 492
M6[a]	256, 320	370, 420, 445	400, 420, 447,[b] 479, 491
M7[a]	246, 256, 292, 325, 350	404, 420	399, 422, 447, 522,[b] 565, 600
P5[a]	256, 282, 290, 324, 340	382, 400, 420, 450, long tail at ca. 500[b]	395, 422, 455,[b] 477, 490, 504, 525
P6[a]	258, 320, 350	380, 400, 420, 488,[b] 530	395, 420, 458,[b] 483, 505, 540
P7[a]	250, 294, 348	404, 420, 540,[b] 565	401, 423, 454, 530,[b] 570, 615

[a] From ref 15. [b] Emission maximum of the 0−0 phosphorescence peak.

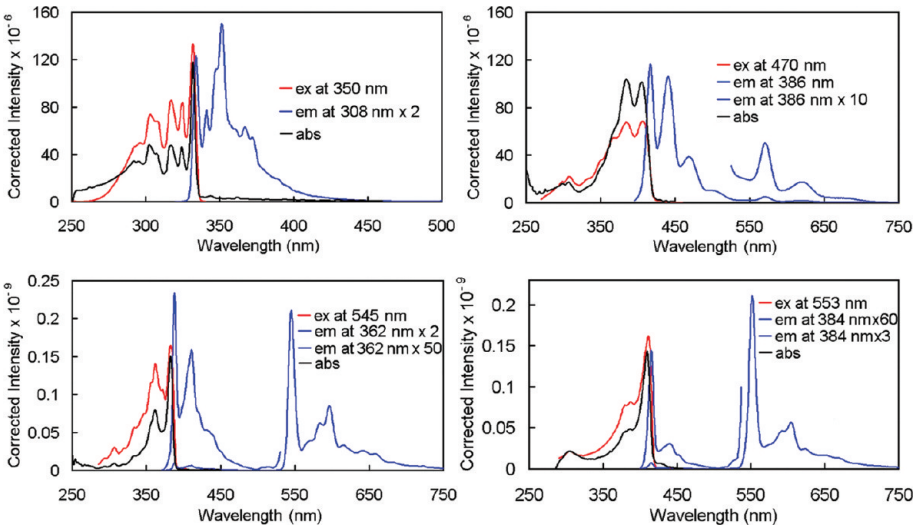

Figure 1. Absorption (black), excitation (red) and emission (blue) spectra of $\mathbf{L_1}$ (top left), **A1** (top right), **M1** (bottom left), and **P1** (bottom right) in 2MeTHF at 77 K.

the other hand, both the diplatinum monomer and its polymer analogue showed fluorescence peaks at 388, 404; 409, 431 nm and phosphorescence signals at 541, 597; 550, 593 nm, respectively.

Emission of 2,7-Carbazole System. The emission spectra measured for diplatinum 2,7-carbazole (**M2**) and its corresponding gold derivative (**A2**) as well as the polymer (**P2**) in 2MeTHF at 77 K are given in Figure 2 and those at 298 K are depicted in the Supporting Information (Figure S2).

The 77 K spectra displayed in Figure 2 show the characteristic fluorescence peaks for the carbazole chromophore at 379, 400, 425; 384, 404; 414, 436 nm for digold (**A2**), diplatinum (**M2**) and diplatinum-2,7-carbazole polymer (**P2**), respectively, whereas the phosphorescence 0−0 emission peaks for the three compounds are detected at 501; 513; 524 nm for **A2**, **M2** and **P2**, respectively. The emission bands for the polymer exhibit a red shift of about 35 nm for the fluorescence λ_{0-0} band and of 23 nm for the λ_{0-0} phosphorescence for **P2** as compared to the diplatinum monomer **M2**. Saliently, the room-temperature (298 K) phosphorescence for the 2,7-carbazole derivatives is more intense than that for their 3,6-carbazole congeners.

The digold 3,6-carbazole (**A3**) and the digold 2,7-carbazole species (**A2**) were studied in order to study the effect of the substitution position on the luminescence properties. The emission spectrum for **A3** recorded in 2MeTHF at 77 K is illustrated in Figure 3.

The fluorescence for the digold 3,6-carbazole compound (**A3**) spreads over the range of the 350−400 nm with the λ_{0-0} fluorescence placed at 381 and 403 nm, whereas the phosphorescence signal at 430−550 nm with $\lambda_{0-0} = 433$ nm. On comparison with the corresponding digold 2,7-carbazole (**A2**) the λ_{0-0} appears at 379 and 400 nm for the fluorescence emission and at 501 nm for the phosphorescence. A red shift was observed for the digold complex bearing 2,7-carbazole as compared to the 3,6-analogue. This shift can be explained

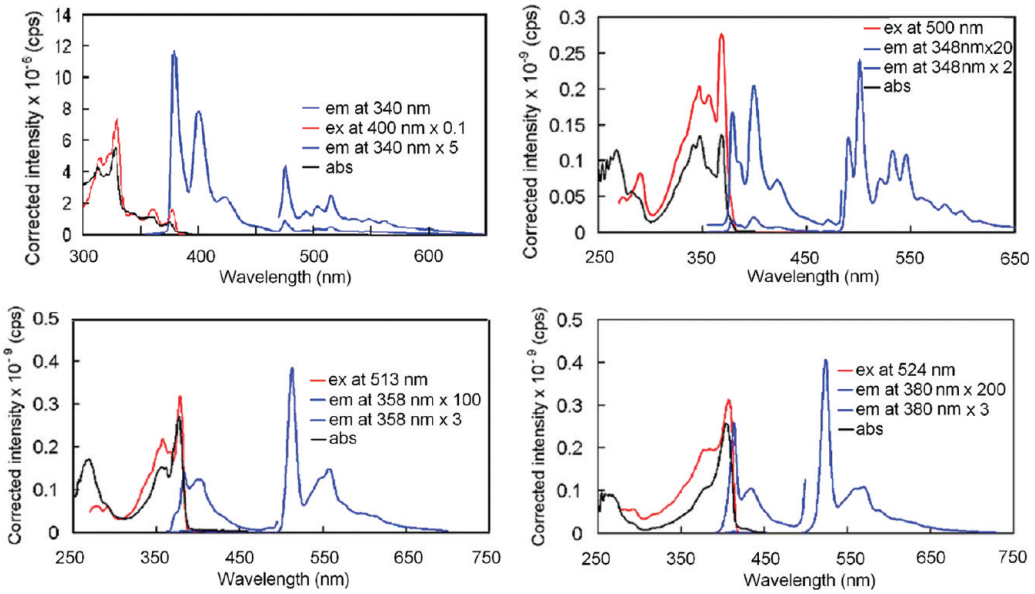

Figure 2. Absorption (black), excitation (red) and emission (blue) spectra of $\mathbf{L_2}$ (top left), **A2** (top right), **M2** (bottom left), and **P2** (bottom right) in 2MeTHF at 77 K.

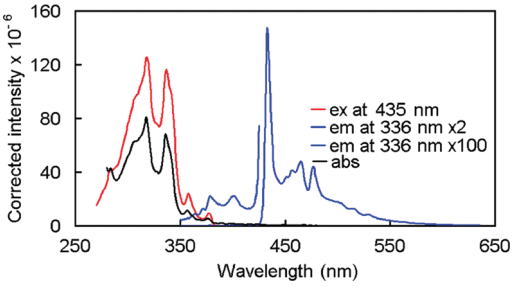

Figure 3. Absorption (black), excitation (red) and emission (blue) spectra of **A3** in 2MeTHF at 77 K.

by considering the reported increased stabilization of the highest occupied molecular orbital (HOMO) of the carbazole upon substitution at the positions 3,6 compared to that substituted at the 2,7 position. This is explained by the greater electron density at the 3,6-positions in comparison with the 2,7 ones.[14d,29]

Dyads and Triads. Mixed-aryl carbazole−fluorene-containing dyads and triads were studied since these types of compounds are prone to S_1 electron and T_1 energy transfers.[13−15]

Dyads. The emission spectra for the carbazole−fluorene dyad ligand ($\mathbf{L_4}$), the digold (**A4**) and the diplatinum (**M4**) analogues in 2MeTHF at 77 K are given in Figure 4.

For the spectrum of the carbazole−fluorene diethynyl ligand $\mathbf{L_4}$, only the fluorescence was observed with vibronic bands located at 384, 398 and 425 sh nm (sh = shoulder). The phosphorescence was also detected for the other metal-containing derivatives, spreading over the range of 530−650 nm, by virtue of the increased intersystem crossing induced by the heavy atom effect. The comparison between the free carbazole and fluorene emissions with that of the mixed compounds is necessary in order to address the changes in the spectra of the mixed aryl species. At 77 K, the fluorescence peaks were observed at 388 and 411 nm for diplatinum 2,7-fluorene (**M1**) (Figure 1) while the diplatinum 2,7-carbazole complex (**M2**) shows the fluorescence signals at 384 and 404 nm (Figure 2). The emission spectra of the mixed carbazole−fluorene compounds (Figure 4) show a strong resemblance to that measured for fluorene alone with no evidence for any fluorescence of the carbazole moiety. The same behavior was noted for the room temperature measurements (Figure S3 in Supporting Information). The carbazole and fluorene longer-lived phosphorescence emissions of the dyads were investigated by time-resolved spectroscopy in the μs time scale in 2MeTHF at 77 K (Figure 5).

The time-resolved spectra given above showed that the strong carbazole phosphorescence at $\sim$ 447 nm is highly quenched in the mixed dyads where it appears only as a weak emission in carbazole−fluorene dyads. This carbazole phosphorescence quenching is even more pronounced in the polymers. This observation suggests that T_1 energy transfer from the carbazole to fluorene unit may be operating. A similar observation was also made for the previously investigated Pt-containing carbazole−fluorene−carbazole systems.[15]

Triads. The luminescence spectra of [Ph−PtL_2−C≡C−**Cz**]$_2$−**X**− where **X** = **Cz** or **F**, and L = PEt_3 were studied previously.[15] The results showed that emission of carbazole trimer exhibits fluorescence features at 400 (sh) and 420 nm while the phosphorescence presents vibronic peaks at 447, 479 and 491 (sh) nm. Here, we report the digold(I) analogue. The luminescence spectra of **A6** and **A7** in 2MeTHF at 77 K are given in Figure 5 and those at 298 K are placed in the Supporting Information (Figure S4).

The spectra in Figure 6 for the mixed carbazole−fluorene−carbazole triad **A7** exhibit a fluorescence band (at 397 and 419 nm) far different in band-shape from that of the carbazole trimer **A6** (at 397 and 416 nm). Moreover, while the cabazole trimer **A6** exhibits a 0−0 phosphorescence peak at 438 nm and vibronic features at 453, 468 (sh), and 483 nm; the mixed triad **A7** shows a distinctively different phosphorescence signal at 445 (sh), 472 (sh), 529, 570, and 610 (sh) nm. The shoulder observed at 445 nm matches the carbazole 0−0 phosphorescence peak and the stronger features observed over the range 527−610 nm is the signature of the fluorene phosphorescence (see Figure 1). The time-resolved spectra in the μs time scale were thus recorded in 2MeTHF at 77 K (Figure 7).

For the time-resolved spectra (and those of Figure 6), based on the comparison between the spectrum recorded for

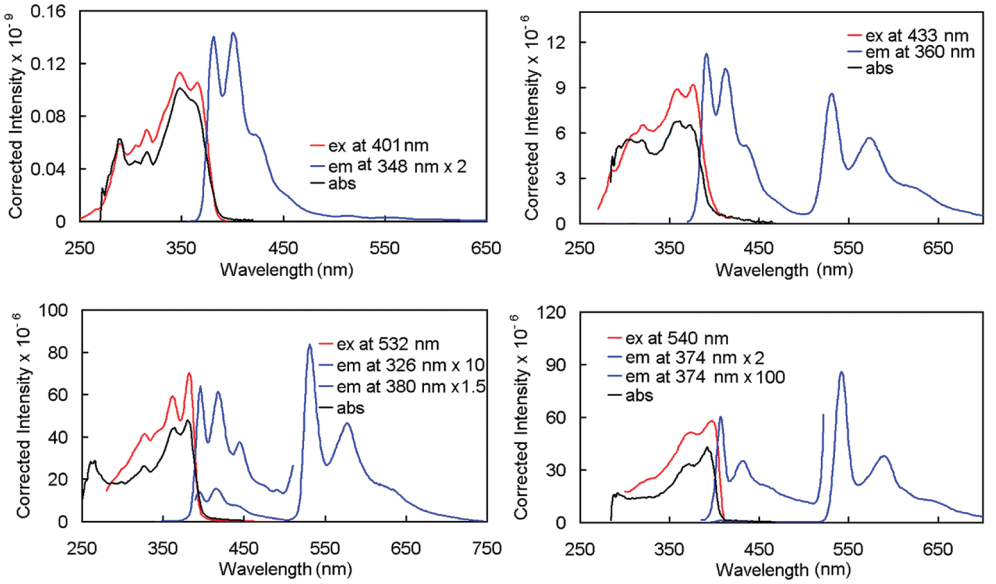

Figure 4. Absorption (black), excitation (red) and emission (blue) spectra of $\mathbf{L_4}$ (top left), **A4** (top right), **M4** (bottom left), and **P4** (bottom right) in 2MeTHF at 77 K.

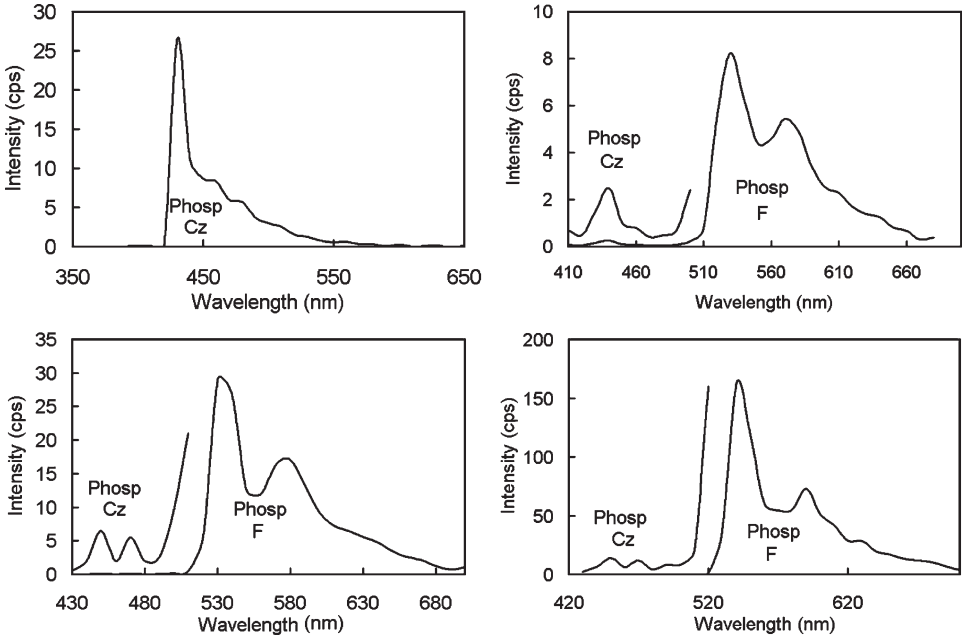

Figure 5. Time-resolved emission spectra of **A3** (top left), **A4** (top right), **M4** (bottom left) and **P4** (bottom right) in 2MeTHF at 77 K in the 10−50 μs time scale. The phosphorescence of carbazole and fluorene chromophores is indicated as Phosp Cz and Phosp F, respectively.

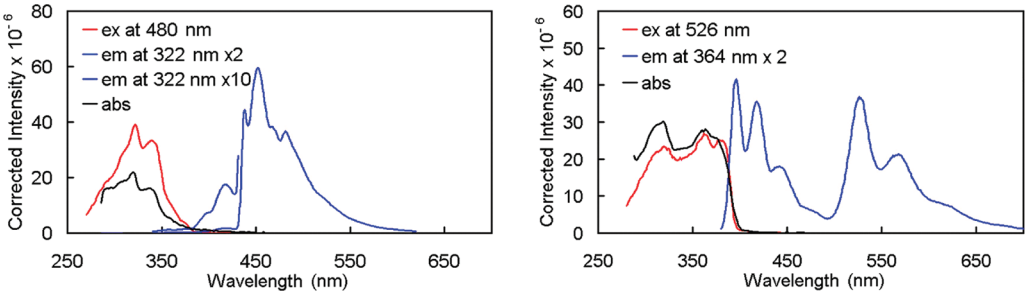

Figure 6. Absorption (black), excitation (red) and emission (blue) spectra of **A6** (left) and **A7** (right) in 2MeTHF at 77 K.

the carbazole trimer and the carbazole−fluorene−carbazole derivative, one can suspect that the phosphorescence of the carbazole has been quenched in the triad system **A7.** This allows us to again suggest the presence of an energy transfer from the higher triplet energy level of the carbazole to the lower fluorene triplet level.

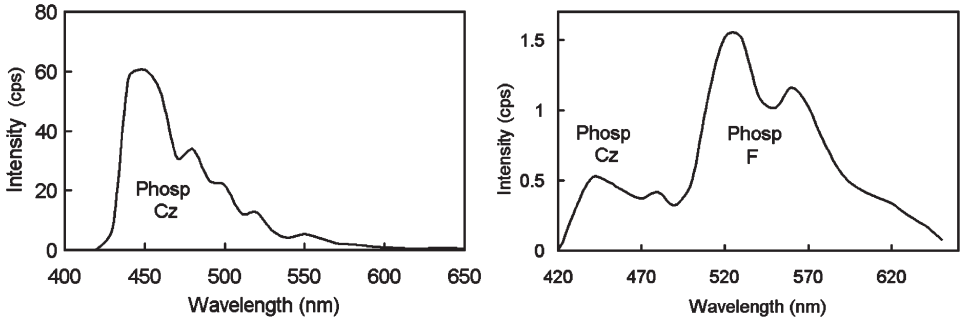

Figure 7. Time-resolved emission spectra of **A6** (left), and **A7** (right) in 2MeTHF at 77 K in the 10−50 μs time scale. The phosphorescence of carbazole and fluorene chromophores is indicated as Phosp Cz and Phosp F, respectively.

Molecular Orbital Calculations and Analyses of the Model Compounds. The nature of the S_1 and T_1 excited states of the model compounds was addressed by density functional theory (DFT) and time-dependent DFT (TDDFT). The molecular orbital (MO) energy diagrams were computed using the optimized geometries in the ground and triplet excited states (see Experimental Section for detail). Figure 8 portrays the relevant MOs describing the lowest energy electronic transitions. A more complete description of selected relevant MOs is provided in the Supporting Information.

The main conclusion of the MO analyses is that the frontier MOs are composed of π-systems of the various aromatics and of atomic orbitals of the Pt metal, so the lowest energy transitions are a variable mixture of $\pi-\pi^*$ and charge transfers (metal-to-ligand charge-transfer, MLCT, and ligand-to-metal charge-transfer, LMCT, where L = carbazole and fluorene). A compound not prepared in this work noted as **Pt-3,6−F−Pt**, where the fluorene is denoted as "**F**", here substituted at the 3 and 6-positions, and "**Pt**" stands for *trans*-Pt$(PMe_3)_2$Ph, was also investigated for comparison purposes. The calculated frontier MOs bear clear resemblance with those for **M3** (i.e., the 3,6-carbazole equivalent), but the MO energies differ as expected. As a result, the lowest energy transition for this case turned out to be high in comparison with the others.

The selected lowest energy singlet−singlet electronic transitions (addressed by TDDFT) are listed and described in Table 2. The computed 0−0 transition energies compare reasonably well to the experimentally observed 0−0 peaks (placed inside parentheses in Table 2).

The nature of the triplet states for **M1** to **M7** was also addressed by DFT by examining the MO description of the highest semioccupied molecular orbital (HSOMO). The approximated position of the phosphorescence was estimated by calculating the energy difference between the HOMO and HSOMO generated from the optimized geometries of the S_1 and T_1 states, respectively. The computational results are presented in Table 3 and Figure 8. The comparison between the experimental and calculated position of the 0−0 phosphorescence peak is reasonable where discrepancies going from 1 to 17 nm are computed.

For all of the investigated compounds, except for **M5** and **M6**, the HSOMO resembles very much that of the LUMO. This indicates that the relaxation of the electron going from the LUMO in the S_1 state down to the HSOMO of the T_1 state does not have a major symmetry constraint to overcome during the process. For **M5** and **M6**, the symmetry-corresponding MOs to the HSOMO's are found at the LUMO+2 and LUMO+1, respectively. The reason for this property is that the LUMO, LUMO+1 and LUMO+2 are placed within 0.02 au Noteworthy, the computed lowest energy S_0-S_1 electronic transitions involve, precisely, the LUMO+2 and LUMO+1 for **M5** and **M6**, respectively. Conversely the other compounds, **M1**, **M2**, **M3**, **M4**, and **M7**, exhibit the LUMO's of the S_1 state that corresponds to the HSOMO of the triplet manifold. So the important conclusion is that the nature of the lowest energy S_1 and T_1 excited states is the same for all cases.

No computation was undertaken for the gold complexes. On the basis of the resemblance of the emission spectra, such an investigation does not appear relevant since similar conclusions are expected.

Emission Lifetimes and Electron and Energy Transfers. The emission lifetimes of all compounds at both 77 and 298 K in 2MeTHF are given in Table 4. The position of the 0−0 emission peaks obtained from the luminescence spectra of the carbazole and fluorene compounds (Table 3) enables us to assign the carbazole to have the upper energy S_1 and T_1 levels (energy donor D) and fluorene to have the lower energy level (energy acceptor A). Indeed, the time-resolved spectra (Figures 5 and 7) show that the phosphorescence emission from the carbazole (at about 430, 450, 450, 450, and 440 nm for **A4**, **M4**, **P4**, **A6**, and **A7**, respectively) is quenched in the dyad and triad. Moreover, the triplet emission lifetimes for the carbazole chromophore in the absence of the acceptor are longer than that for the mixed carbazole−fluorene dyads and triads (Table 4). This is supported by the transient absorption spectra (below) indicating that only T_1 species are observed. So, electron transfers from T_1 are excluded, and only the energy transfer from **Cz** to **F** explains the decrease in phosphorescence intensity and lifetime.

On the other hand, the time-resolved fluorescence emission for the studied dyads **A4**, **M4**, and **P4** and triad **A7** was measured and the spectra are given in Figure 9. Those for **M7** and **P7** are known in the literature.[15] A careful examination of the fluorescence traces while exciting the samples at 350 nm (i.e., in the absorption bands of both chromophores **Cz** and **F**) at different delay times ranging from 43.5 ns (the very early stage of the excitation laser pulse) through the maximum of the laser signal at 45 ns, and then at 46 ns, shows that the band shape is constant at all time meaning that only one species is detected. The vibronic signature and 0−0 position observed in Figure 9 indicate the presence of the fluorene fluorescence only. The carbazole fluorescence is found to be totally quenched.

Similarly, the same time-resolved fluorescence spectra recorded at 298 K show exactly the same behavior (i.e., no carbazole fluorescence). This behavior is explained by the presence of a photoinduced electron transfer from the carbazole chromophore in its S_1 state to the fluorene, as previously demonstrated for other carbazole/fluorene-containing organometallic oligomer and polymer (**M7** and **P7**) based on a combination of spectroscopic and electrochemical findings.[15]

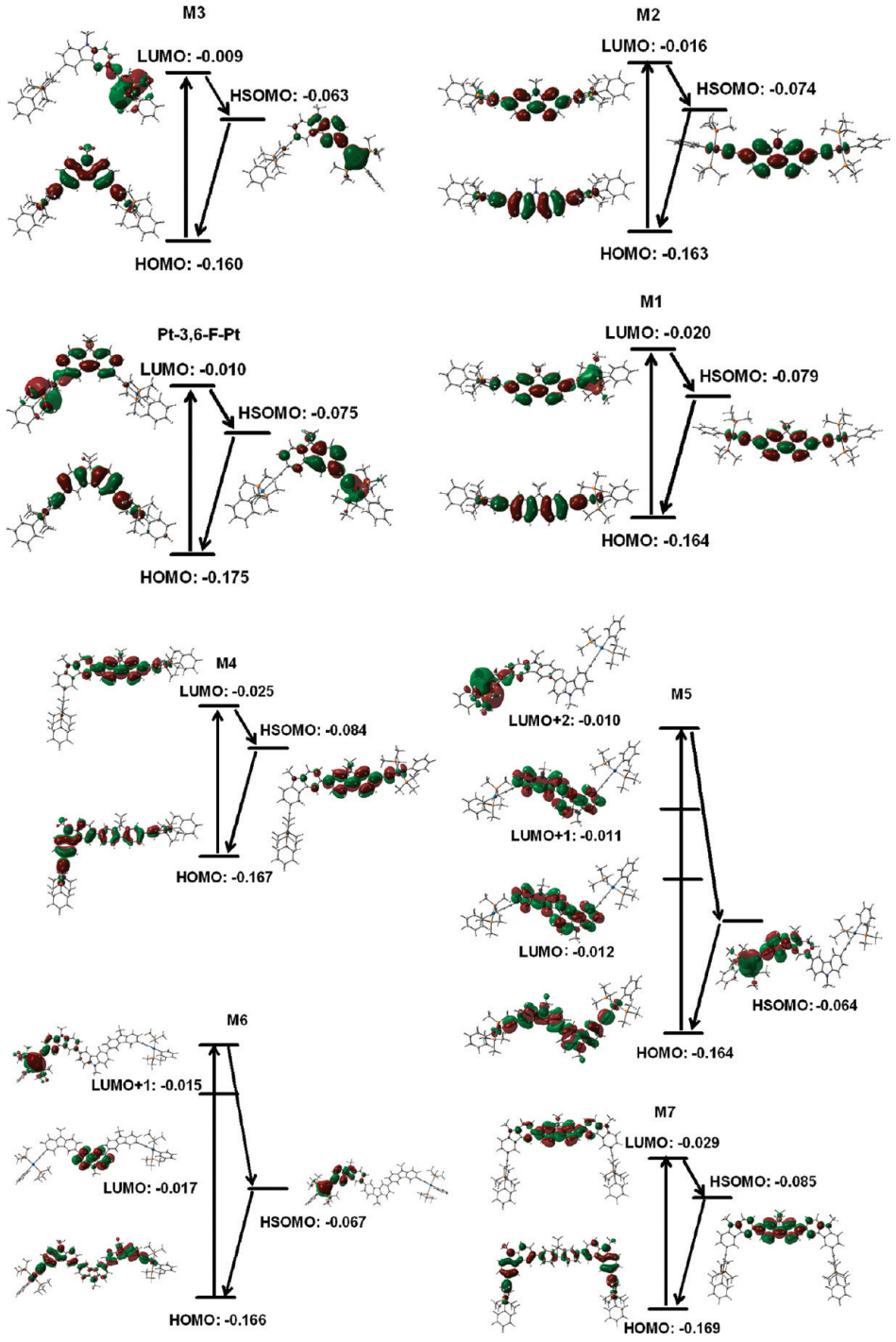

Figure 8. Representations of the frontier MOs for **M1**−**M7** and the hypothetical molecule **Pt-3,6**−**F**−**Pt**.

Moreover, the excitation spectrum of the mixed carbazole/fluorene dyads (**A4** and **M4**) and triad (**A7**) were measured as a function of the emission wavelength (Figure 10). The excitation spectra exhibit differences between the monitoring across the fluorene fluorescence and phosphorescence bands. Indeed, the excitation spectra monitored across the fluorescence band exhibit a red-shifted signature associated with fluorene only (based upon a comparison with the absorption spectra of only fluorene-containing compounds included in Chart 1). This means that excitation in the carbazole absorption band does not lead to fluorene fluorescence, consistent with an electron transfer mechanism.

On the other hand, the monitoring of the fluorene phosphorescence gives rise to excitation spectra that exhibit a blue-shifted signature attributable to the carbazole chromophore (again based upon the comparison with absorption spectra of only carbazole-containing compounds (Chart 1)). This means that the occurrence of the strong fluorene phosphorescence is due to a T_1 energy transfer from the carbazole chromophore to fluorene. This process is aided by the heavy atom effect where a Pt or Au atom is linked to the carbazole aromatics, hence efficiently populating their triplet excited states.

The transient spectra of **A2** and **M2** (two compounds containing only the 2,7-carbazole aromatic unit) exhibit absorptions centered at 640 and 680 nm, respectively, in a 6−80 μs time scale (Figure 11). Because these compounds are not composed of an electron donor and acceptor, the

Table 2. Calculated Lower Transition Energies and Major Contributions for the Lowest Energy Transitions

	λ/nm (exptl value)	oscillator strength	composition (relative contribution)
M1	358 (374)	1.573	HOMO → LUMO (82%)
M2	345 (376)	0.481	HOMO → LUMO (42%), HOMO → LUMO+2 (46%)
M3	350 (345)	0.115	HOMO-1 → LUMO (10%), HOMO → LUMO (85%)
Pt-3,6−F−Pt	323	0.010	HOMO-1 → LUMO+1 (20%), HOMO-1 → LUMO+2 (16%), HOMO → LUMO+2 (48%)
	322	0.023	HOMO-1 → LUMO+1 (18%), HOMO-1 → LUMO+2 (14%), HOMO → LUMO+1 (48%)
	306	0.077	HOMO → LUMO (54%), HOMO → LUMO+2 (14%), HOMO → LUMO+3 (12%)
	301	0.047	HOMO-1 → LUMO (70%)
M4	355 (364)	1.195	HOMO → LUMO (90%)
	333	0.160	HOMO-1 → LUMO (42%), HOMO-1 → LUMO+2 (24%), HOMO → LUMO+2 (23%)
	324	0.743	HOMO-1 → LUMO (44%), HOMO-1 → LUMO+2 (22%), HOMO → LUMO+2 (22%)
	355	1.195	HOMO → LUMO (90%)
M5	342 (325)[a]	0.160	HOMO-1 → LUMO+2 (16%), HOMO-1 → LUMO+2 (18%), HOMO → LUMO+2 (51%)
	311	1.00	HOMO → LUMO+4 (69%)
M6	345 (320)[a]	0.842	HOMO-1 → LUMO+1 (38%), HOMO → LUMO+1 (53%)
M7	363 (350)[a]	0.924	HOMO → LUMO (93%)

[a] From ref 15.

Table 3. Computed HOMO and HSOMO Energies and Positions of the 0−0 peak in the Phosphorescence Emission

compounds	HOMO energy (au)	HSOMO energy (au)	calculated 0−0 transition energy (nm)[a]	experimental 0−0 transition energy (nm) at 298 K[b]
M1	−0.164	−0.079	536	541 (545)
M2	−0.163	−0.074	512	522 (513)
M3	−0.160	−0.063	470	n.d.[d] (450)
Pt-3,6−F−Pt	−0.175	−0.075	456	
M4	−0.167	−0.084	549	544 (532)
M5	−0.164	−0.064	456	n.d. (446)[c]
M6	−0.166	−0.067	460	n.d. (447)[c]
M7	−0.169	−0.085	542	n.d. (522)[c]

[a] Calculated from the energy difference between the HOMO and HSOMO. [b] The data at 77 K are shown in parentheses for comparison. [c] These data for **M5**−**M7** are taken from ref 15. [d] n.d. = not detected at 298 K.

Table 4. Emission Lifetimes in 2MeTHF at 77 and 298 K

	lifetime (λ)[a]				Φ[b]	
	77 K		298 K			
	fluorescence (ns)	phosphorescence (μs)	fluorescence (ns)	phosphorescence (μs)	Φ_F	Φ_P
L_1	0.88 ± 0.01 (350 nm)	[c]	0.71 ± 0.02 (350 nm)	*c*	0.91	*c*
A1	0.29 ± 0.02 (417 nm)	[c]	0.18 ± 0.03 (411 nm)	*c*	0.62	*c*
M1	0.37 ± 0.01 (411 nm)	258 ± 1 (545 nm)	0.11 ± 0.01 (385 nm)	84 ± 1 (546 nm)	0.019	0.031
P1	0.31 ± 0.06 (416 nm)	154 ± 1 (553 nm)	0.23 ± 0.04 (355 nm)	19.4 ± 0.7 (550 nm)	0.011	0.028
L_2	13.2 ± 0.4 (400 nm)	4.26 ± 0.06 (475 nm)[d]	7.3 ± 0.2 (400 nm)	*c*	0.73	*c*
A2	0.30 ± 0.02 (385 nm)	828 ± 4 (491 nm)	0.14 ± 0.02 (380 nm) 0.13 ± 0.01 (398 nm)	128 ± 1 (509 nm)	0.026	0.074
M2	0.32 ± 0.01 (383 nm)	398 ± 3 (513 nm)	0.13 ± 0.02 (387 nm)	10.6 ± 0.2 (522 nm)	0.0094	0.022
P2	0.26 ± 0.04 (380 nm)	111.7 ± 0.6 (434 nm)	0.085 ± 0.030 (409 nm) 0.080 ± 0.012 (428 nm)	55.3 ± 0.3 (526 nm)	0.0041	0.025
L_3	12.9 ± 0.4 (385 nm)	3.5 ± 0.3 (445 nm)[d]	7.0 ± 0.1 (385 nm)		0.68	
A3	0.24 ± 0.03 (396 nm)	201 ± 0.3 (450 nm)	0.17 ± 0.01 (396 nm)		0.011	
M3	0.43 ± 0.07 (405 nm)	525 ± 2.9 (460 nm)	0.13 ± 0.03 (401 nm)	19.84 ± 0.66 (437 nm)	0.0052	0.0244
P3	0.35 ± 0.04 (420 nm)	46.2 ± 0.5 (460 nm)	0.15 ± 0.030 (415 nm)		0.011	
L_4	2.56 ± 0.15 (350 nm) 2.67 ± 0.13 (387 nm)	[c]	2.2 ± 0.2 (406 nm)	*c*	0.77	*c*
A4	0.62 ± 0.13 (414 nm) 0.22 ± 0.02 (390 nm)	1594 ± 14 (530 nm) 330 ± 26 (450 nm)	0.70 ± 0.08 (405 nm)	*c*	0.20	*c*
M4	0.15 ± 0.02 (396 nm) 0.30 ± 0.03 (417 nm)	71.4 ± 2.6 (445 nm) 618 ± 5 (532 nm)	0.13 ± 0.02 (420 nm)	220 ± 5 (543 nm)	0.017	0.012
P4	0.13 ± 0.01 (407 nm) 0.44 ± 0.02 (430 nm)	32.4 ± 0.2 (455 nm) 391 ± 3 (540 nm)	0.09 ± 0.01 (420 nm)	315 ± 5 (543 nm)	0.0021	0.016
A5	0.48 ± 0.04 (415 nm) 0.46 ± 0.06 (395 nm)	774 ± 11 (450 nm)	0.43 ± 0.01 (417 nm)	*c*	0.053	
M5[e]	0.340 ± 0.050 (410 nm)	147 ± 3 (446 nm)	0.16 ± 0.05 (417 nm)	*c*	−	*c*
A6	0.72 ± 0.03 (420 nm) 0.22 ± 0.02 (397 nm)	1057 ± 5 (450 nm)	0.54 ± 0.05 (418 nm)	*c*	0.075	
M6[e]	0.350 ± 0.025 (400 nm)	149 ± 2 (447 nm)	0.13 ± 0.04 (420 nm)	*c*	−	*c*
A7	0.66 ± 0.17 (420 nm) 0.15 ± 0.01 (395 nm)	804 ± 17 (525 nm) 515 ± 20 (450 nm)	0.63 ± 0.18 (417 nm)	*c*	0.17	
M7[e]	not observed	132 ± 6 (450 nm)	0.12 ± 0.01 (400 nm)	*c*	−	*c*

[a] The wavelength for monitoring the lifetime is shown in parentheses. [b] The quantum yield was measured in 2MeTHF at 298 K using 9,10-diphenylanthracene as the reference ($\Phi_F = 1.0$)[14] and $\lambda_{ex} = 320$ nm. [c] No phosphorescence signal was observed. [d] Phosphorescence lifetime for **L_2** and **L_3** was given in s. [e] From ref [15].

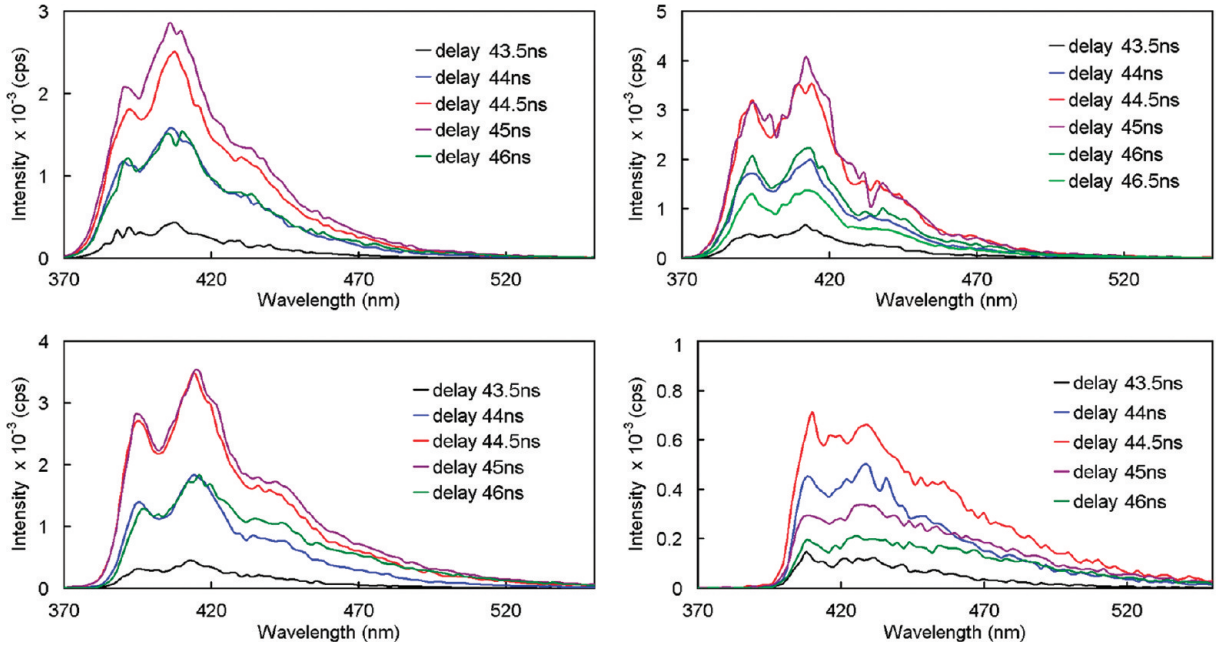

Figure 9. Time-resolved fluorescence spectra of **A4** (top left), **A7** (top right), **M4** (bottom left), and **P4** (bottom right) in 2-MeTHF at 77 K. The time delays are indicated on the graphs and correspond to the rising time of the laser pulse where the delay time of 43.5 ns is the beginning of the laser pulse and delay time of 45 ns is the pulse maximum (λ_{exc} = 350 nm). The pulse width at half-maximum is 1.3 ns.

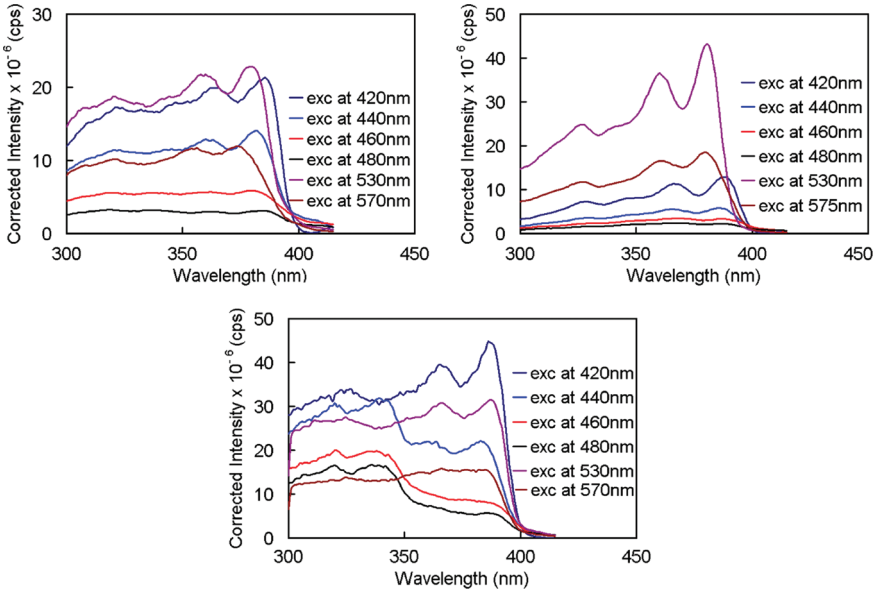

Figure 10. Excitation spectra of **A4** (top left), **M4** (top right), and **A7** (bottom) in 2MeTHF at 77 K monitored at different wavelengths.

possibility of a photoinduced electron transfer is excluded. So, these two absorptions are the fingerprint of T_1-T_n absorptions.

The transient absorption spectra for the mixed carbazole–fluorene dyads, triads, and polymers (**A4**, **M4**, **P4**, **A7**) were measured in 2MeTHF at 77 K for comparison (Figure 12). The corresponding room temperature transient spectra are provided in Figures S5 and S6. The comparison between the transient spectra presented in Figures 11 and 12 is clear. All these species exhibit only the transient absorption located between 640 and 680 nm, with no evidence for new species, notably that of the carbazole radical cation (770–870 nm).[30] So, the only possible species observed at time scale exceeding 13 ns (pulse width of the laser pump) are the triplet carbazoles and fluorenes since they absorb in the same range ($T_1 \rightarrow T_n$).

Rates for Energy and Electron Transfers. The phosphorescence lifetimes were analyzed in the context of triplet energy transfers, and their rates, k_{ET}, at 77 K were extracted using eq 1:[31]

$$k_{ET} = \left(\frac{1}{\tau_e} - \frac{1}{\tau_e^0}\right) \quad (1)$$

where τ_e^0 is the emission lifetime for the donor in a structurally related molecule where no energy transfer takes place (a comparison molecule here), and τ_e is the emission lifetime of the donor in the dyad or triad. Compound **A5** was used as the comparison molecule for dyad **A4** and tricarbazole **A6** was the homologue for triad **A7**. Moreover, for dyad **M4** and polymer **P4**, the comparison molecule and polymer are **M5** and **P5**, etc.[15] The k_{ET} values are given in Table 5.

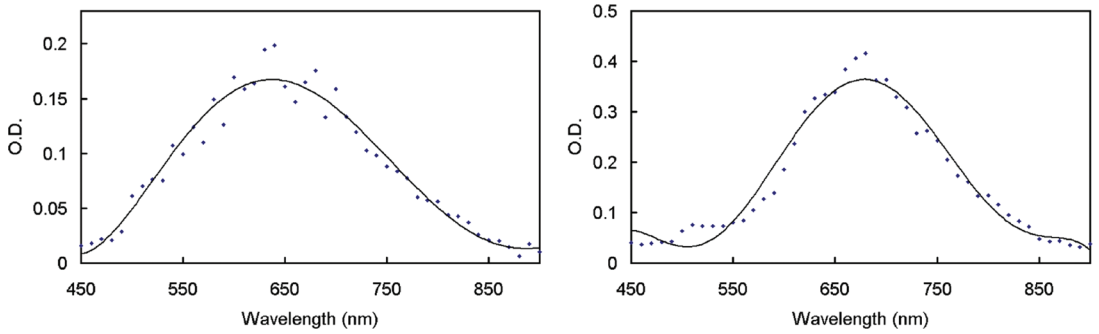

Figure 11. Transient spectra of **A2** (left) and **M2** (right) in 2MeTHF at 77 K excited at 355 nm in the 8−60 μs time scale.

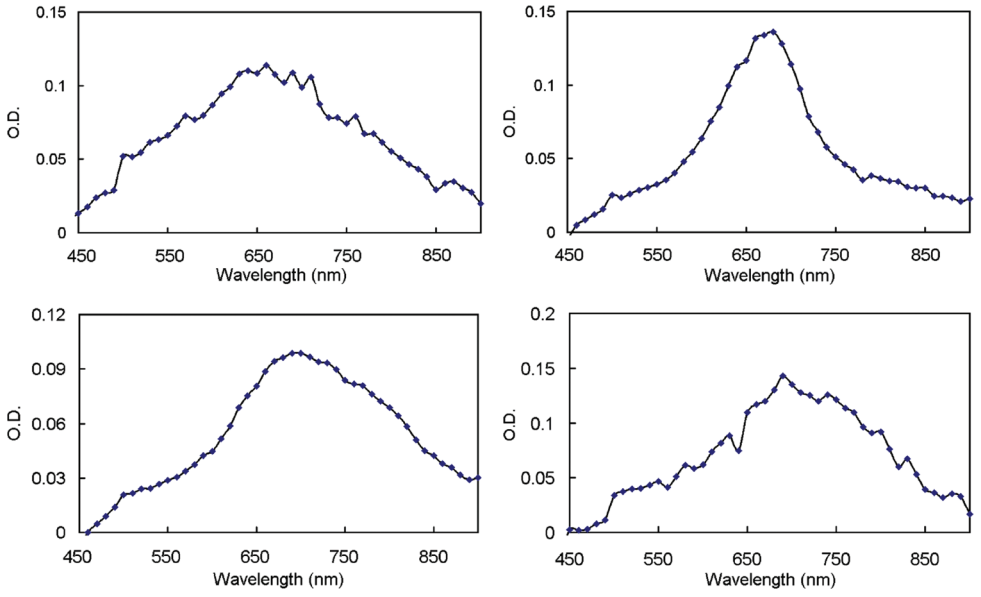

Figure 12. Transient spectra of **A4** (top left), **M4** (top right), **P4** (bottom left), and **A7** (bottom right) in 2MeTHF at 77 K excited at 355 nm in the 8−60 μs time scale.

Table 5. Rates for Triplet Energy Transfer (k_{ET}) at 77 K and Singlet Electron Transfer (k_{et}) at 298 and 77 K for A4, M4, P4, A7, M7, and P7 in 2MeTHF

	77 K		
compounds or polymer	singlet k_{et} (s^{-1})	triplet k_{ET} (s^{-1})	298 K singlet k_{et} (s^{-1})
A4	$> 2.4 \times 10^9$	1.7×10^3	$> 12 \times 10^{11}$
M4	$> 3.6 \times 10^9$	7.3×10^3	$> 20 \times 10^{11}$
P4	$> 3.9 \times 10^9$	14.8×10^3	$> 4 \times 10^{11}$
A7	$> 2.2 \times 10^9$	1.0×10^3	$> 14 \times 10^{11}$
M7[a]	*b*	1.9×10^3	$> 10 \times 10^{11}$
P7[a]	*b*	3.4×10^3	$> 4 \times 10^{11}$

[a] From ref 15. [b] Not evaluated.

First of all, the rates reported in Table 5 range ca. 10^3-10^4 s^{-1}. This magnitude is considered slow but not unusual for energy transfer in the triplet states. The k_{ET} value for the digold dyad, **A4** (1.7×10^3 s^{-1}), is lower than that found for the diplatinum analogue, **M4** (7.3×10^3 s^{-1}). The k_{ET} value for dyad **M4** and the corresponding polymer **P4** (14.8×10^3 s^{-1}) are also different. The slower rate for triplet energy transfer in the dyad compared to the polymer is consistent with the fact that in the dyad the donor is situated beside one acceptor chromophore, whereas in the polymer, the same donor is flanked by two acceptors. So the probability of transfer is increased by a factor of 2. The experimental data reflect just that (7.3 vs 14.8×10^3 s^{-1}). In fact, we find that k_{ET} varies as **A4** < **M4** < **P4** and **A7** < **M7** < **P7**, where the ratio of 1:2 is also seen between **M7** and **P7**. Also, the Pt-containing species exhibit much stronger phosphorescence intensity vs fluorescence with respect to the Au-analogue. These two observations indicate that the triplet states are better populated by the Pt atom in these cases.

The k_{ET} values agree with those previously reported for other triplet energy transfer systems,[15,32] but at the same time these values lie on the lower end of the literature data.[32] The reason for this can be explained on the basis of the nonzero dihedral angle between carbazole donor and fluorene acceptor (see X-ray data in Supporting Information : 8.0° for 3-(2-bromo-9,9-dibutylfluoren-7-yl)-9-butylcarbazole and 37.8° for 3-bromo-6-(2-bromo-9,9-dibutylfluoren-7-yl)-9-butylcarbazole). The rate for triplet energy transfer is hence anticipated to decrease since the only operating mechanism for transfer is the double electron exchange (Dexter mechanism). So, this process requires a good D−A orbital overlap,[32] and a decrease in π-conjugation from a larger dihedral angle should decrease this overlap, and consequently, the rate.

An interesting feature is the comparison of the series **A4**, **M4**, **P4** vs **A7**, **M7**, **P7**. Indeed, the series of **A7**, **M7** and **P7** exhibits twice the amount of **Cz** units (leading to a higher concentration of T_1 state species) and twice **Cz** units (leading to a larger number of antenna molecules) per **F** chromophore, k_{ET} should be intuitively be larger than the corresponding

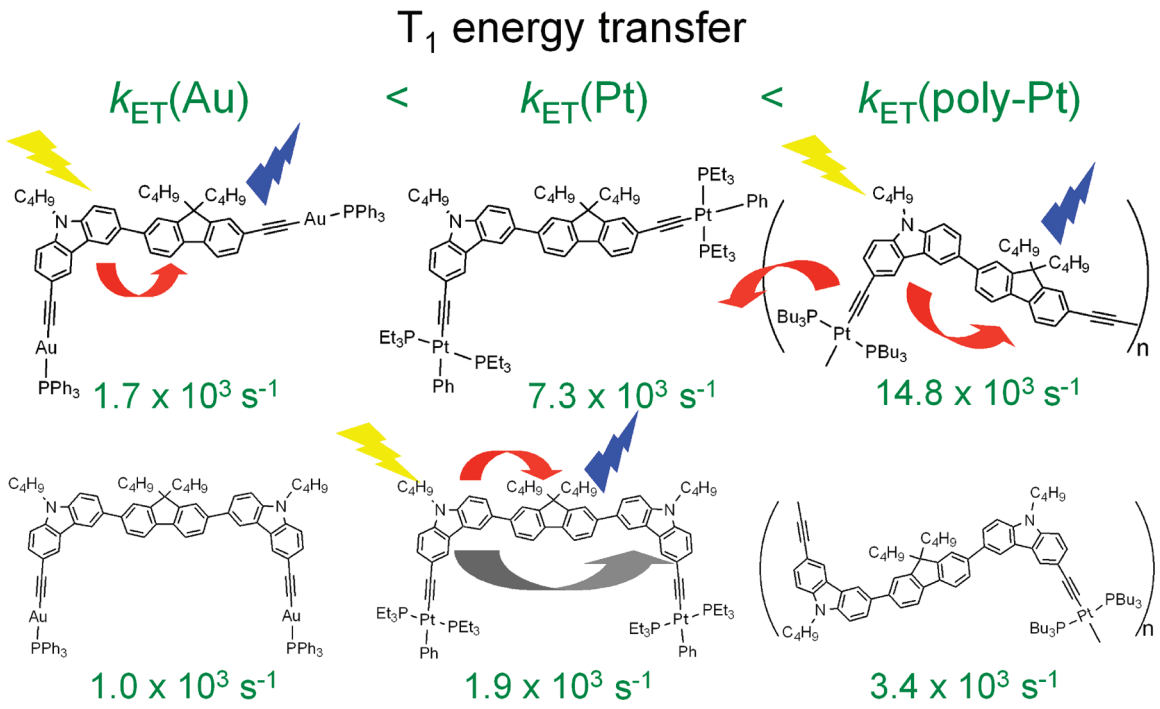

Figure 13. Relationship between the structures and the rates for **A4**, **M4**, **P4**, **A7**, **M7** and **P7**. The red arrows represent T_1 energy transfer whereas the gray one represents excitation energy delocalization.

congeners. The reverse is observed, meaning that an extra competitive nonradiative process takes place. The increase in internal conversion from the T_1 state due to the increase in number of vibrational levels available for relaxation can be ruled out since the rates are double (i.e., an increase in k_{ET}, not a decrease) in the polymers vs the dyads and triads. So, the competitive process could be a delocalization of the excitation energy over identical chromophores (i.e., exciton, see gray arrow in Figure 13). Then each individual chromophore that shares this excitation increases the probability for nonradiative relaxation. This is a possible explanation, but the exciton phenomenon is well-known in nature.[33]

In this work, the accurate evaluation of the rate for photoinduced electron transfer, k_{et}, (^{1}**Cz*** → **F**) is not possible due to the absence of carbazole fluorescence. So in the absence of a sub ps or ps laser transient absorption spectrometer to monitor the risetime of the cations and anions during the photoinduced electron transfer, the lower limit of the rates can be estimated by using the limit of our emission detection ($\Phi_F < 0.0001$). Indeed, with the equation $k_{et} = (\Phi_F^0/\tau_F^0)\,[(1/\Phi_F) - (1/\Phi_F^0)]$,[31] where Φ_F and Φ_F^0 are the fluorescence quantum yields for the donor in the dyad (D−A) and the model compound where no electron transfer takes place, lower limits for k_{et} are extracted. The model compounds used are **A5** and **A6** for dyad **A4** and triad **A7**, respectively, whereas for dyad **M4** and polymer **P4**, the comparison model compound and polymer are **M5** and **P5**, respectively.[15] The estimated lower limits (Table 5) are comparable with what we recently published for similar systems.[15] These lower limits indicate that these transfers must be fast and compare favorably with other systems. We find that the lower limits are slower at 77 K than that at 298 K. This is because that the measurable emission quantum yields are larger and the lifetimes are longer. If the fluorescence lifetime of the donor is longer, then the rate for electron transfer is slower at 77 K. This analysis is speculative but is consistent with a much larger reorganization energy in solid glasses in comparison with fluid solution.

Concluding Remarks

This work reports the preparation and characterization of several new Pt- and Au-containing carbazole−fluorene dyads and triads. As expected, the heavy metal effect is felt upon the observation of an increased intensity of the phosphorescence of the aromatics. This increase in triplet emission quantum yields gave us an opportunity to measure the rate for energy transfer and make a comparison between Pt- and Au-containing species; two metals of very close dimension. We find that the Pt-containing species give rise to faster rates. One possible explanation for this is that the population of triplet excited state is somewhat larger for the Pt species. Again, this explanation is still tentative since the structure about the metal centers is different (square planar vs linear). Moreover, we find that the Pt-complexes exhibit slower T_1 k_{ET}'s than the Pt-polymers. This is explained by the presence of two acceptors flanking the excited donor within the polymer chain, hence offering two pathways to energy transfer. In addition, we also find that T_1 k_{ET} (^{3}**Cz*** → **F**) is slower when the number of Pt/carbazole-containing group is larger. This is tentatively explained by the presence of a competitive process, i.e. excitation energy delocalization over identical chromophores here. We feel that more examples are needed to confirm this hypothesis (only three examples in this work). These findings are important for the design of conjugated organometallic polymers bearing the necessary optical and photophysical properties for photonic devices. The total quenching of the fluorescence of the carbazole chromophore in the dyads and triads, for both Pt and Au species indicates efficient electron transfer processes, with rates exceeding 10^9 s^{-1}. This property too is interesting for the design of conjugated organometallic materials potentially useful in photovoltaic cells for example.

Acknowledgment. This research was supported by a GRF grant from the Hong Kong Research Grants Council (Grant

No: HKBU 202607), Hong Kong Baptist University (FRG/07-08/II-65), and the Natural Sciences and Engineering Research Council of Canada.

Supporting Information Available: Text containing an experimental section, tables of X-ray crystal data for some 3,6-carbazole−2,7-fluorene (di)bromo precursors, and figures showing the absorption, excitation and emission spectra of various metal diynes and polyynes at 298 K, tables of calculated lower transition energies along with their major contributions and figures showing selected frontier MOs for **M1**−**M7**. This material is available free of charge via the Internet at http://pubs.acs.org.

References and Notes

(1) (a) Chou, P.-T.; Chi, Y. *Chem.—Eur. J.* **2007**, *13*, 380. (b) Holder, E.; Langeveld, B. M. W.; Schubert, U. S. *Adv. Mater.* **2005**, *17*, 1109. (c) Wong, W.-Y. *Coord. Chem. Rev.* **2005**, *249*, 971. (d) Baldo, M. A.; Thompson, M. E.; Forrest, S. R. *Pure Appl. Chem.* **1999**, *71*, 2095. (e) Evans, R. C.; Douglas, P.; Winscom, C. J. *Coord. Chem. Rev.* **2006**, *250*, 2093. (f) Wong, W.-Y. *Macromol. Chem. Phys.* **2008**, *209*, 14. (g) Wong, W.-Y.; Wang, X.-Z.; He, Z.; Djurišić, A. B.; Yip, C.-T.; Cheung, K.-Y.; Wang, H.; Mak, C. S. K.; Chan, W.-K. *Nat. Mater.* **2007**, *6*, 521. (h) Wong, W.-Y.; Wang, X.-Z.; He, Z.; Chan, K.-K.; Djurišić, A. B.; Cheung, K.-Y.; Yip, C.-T.; Ng, A. M.-C.; Xi, Y. Y.; Mak, C. S. K.; Chan, W.-K. *J. Am. Chem. Soc.* **2007**, *129*, 14372.

(2) (a) Wong, W.-Y. *Coord. Chem. Rev.* **2006**, *250*, 2627. (b) Wong, W.-Y. *Dalton Trans.* **2007**, 4495. (c) Wong, W.-Y. *J. Inorg. Organomet. Polym. Mater.* **2005**, *15*, 197. (d) Manners, I. *Synthetic Metal-Containing Polymers*; Wiley: Weinheim, Germany, 2004. (e) Long, N. J.; Williams, C. K. *Angew. Chem., Int. Ed.* **2003**, *42*, 2586.

(3) (a) Brédas, J. L.; Cornil, J.; Heeger, A. J. *Adv. Mater.* **1996**, *8*, 447. (b) *Primary Photoexcitations in Conjugated Polymers: Molecular Exciton vs Semiconductor Band Model*; Sariciftci, N. S., Ed.; World Scientific: Singapore, 1997.

(4) (a) Wilson, J. S.; Dhoot, A. S.; Seeley, A. J. A. B.; Khan, M. S.; Köhler, A.; Friend, R. H. *Nature* (*London*) **2001**, *413*, 828. (b) Köhler, A.; Wilson, J. S.; Friend, R. H. *Adv. Mater.* **2002**, *14*, 701. (c) Lupton, J. M.; Pogantsch, A.; Piok, T.; List, E. J. W.; Patil, S.; Scherf, U. *Phys. Rev. Lett.* **2002**, *89*, 167401. (d) Romanovskii, Y. V.; Gerhard, A.; Schweitzer, B.; Scherf, U.; Personov, R. I.; Bassler, H. *Phys. Rev. Lett.* **2000**, *84*, 1027. (e) Dhoot, A. S.; Greenham, N. C. *Adv. Mater.* **2002**, *14*, 1834. (f) Gong, X.; Ostrowski, J. C.; Bazan, G. C.; Moses, D.; Heeger, A. J.; Liu, M. S.; Jen, A. K.-Y. *Adv. Mater.* **2003**, *15*, 45.

(5) (a) Ho, P. K. H.; Kim, J. S.; Burroughes, J. H.; Becker, H.; Li, S. F. Y.; Brown, T. M.; Cacialli, F.; Friend, R. H. *Nature* (*London*) **2000**, *404*, 481. (b) Cao, Y.; Parker, I. D.; Yu, G.; Zhang, C.; Heeger, A. J. *Nature* (*London*) **1999**, *397*, 414. (c) Baldo, M. A.; O'Brien, D. F.; You, Y.; Shoustikov, A.; Sibley, S.; Thompson, M. E.; Forrest, S. R. *Nature* (*London*) **1998**, *395*, 151. (d) Baldo, M. A.; Thompson, M. E.; Forrest, S. R. *Nature* (*London*) **2000**, *403*, 750.

(6) (a) Chao, H.-Y.; Lu, W.; Li, Y.; Chan, M. C. W.; Che, C.-M.; Cheung, K.-K.; Zhu, N. *J. Am. Chem. Soc.* **2002**, *124*, 14696. (b) Lu, W.; Xiang, H.-F.; Zhu, N.; Che, C.-M. *Organometallics* **2002**, *21*, 2343. (c) Ahrens, B.; Choi, K.-H.; Khan, M. S.; Li, P.; Raithby, P. R.; Wilson, P. J.; Wong, W.-Y. *CrystEngComm.* **2002**, *4*, 405. (d) Wong, W.-Y.; Choi, K.-H.; Lu, G.-L.; Shi, J.-X.; Lai, P.-Y.; Chan, S.-M.; Lin, Z. *Organometallics* **2001**, *20*, 5446.

(7) (a) Wong, W.-Y. *Coord. Chem. Rev.* **2007**, *251*, 2400. (b) Wong, W.-Y.; Liu, L.; Shi, J.-X. *Angew. Chem., Int. Ed.* **2003**, *42*, 4064. (c) Zhou, G.; Wong, W.-Y.; Ye, C.; Lin, Z. *Adv. Funct. Mater.* **2007**, *17*, 963. (d) Zhou, G.; Wong, W.-Y.; Lin, Z.; Ye, C. *Angew. Chem., Int. Ed.* **2006**, *45*, 6189. (e) Wong, W.-Y.; Choi, K.-H.; Lu, G.-L.; Lin, Z. *Organometallics* **2002**, *21*, 4475.

(8) (a) Xiao, X.; Fu, Y.; Sun, M.; Li, L.; Bo, Z. *J. Polym. Sci., A: Polym. Chem.* **2007**, *45*, 2410. (b) Li, W.; Qiao, J.; Duan, L.; Wang, L.; Qiu, Y. *Tetrahedron* **2007**, *63*, 10161. (c) Shao, H.; Chen, X.; Wang, Z.; Lu, P. *J. Luminesc.* **2007**, *127*, 349. (d) Liu, R.; Xiong, Y.; Zeng, W.; Wu, Z.; Du, B.; Yang, W.; Sun, M.; Cao, Y. *Macromol. Chem. Phys.* **2007**, *208*, 1503. (e) Yuan, M. C.; Shih, P. I.; Chien, C. H.; Shu, C. F. *J. Polym. Sci., Part A: Polym. Chem.* **2007**, *45*, 2925. (f) Zhen, H.; Luo, J.; Yang, W.; Chen, Q.; Ying, L.; Zou, J.; Wu, H.; Cao, Y. *J. Mater. Chem.* **2007**, *17*, 2824. (g) Kruzinauskiene, A.; Matoliukstyte, A.; Michaleviciute, A.; Grazulevicius, J. V.; Musnickas, J.; Gaidelis, V.; Jankauskas, V. *Synth. Met.* **2007**, *157*, 401. (h) Park, J. H.; Cho, N. S.; Jung, Y. K.; Cho, H. J.; Shim, H. K.; Kim, H.; Lee, Y. S. *Org. Electron.* **2007**, *8*, 272. (i) Zhang, K.; Chen, Z.; Zou, Y.; Yang, C.; Qin, J.; Cao, Y. *Organometallics* **2007**, *26*, 3699. (j) Grisorio, R.; Mastrorilli, P.; Nobile, C. F.; Romanazzi, G.; Suranna, G. P.; Gigli, G.; Piliego, C.; Ciccarella, G.; Cosma, P.; Acierno, D.; Amendola, E. *Macromolecules* **2007**, *40*, 4865. (k) Liu, Q. D.; Lu, J.; Ding, J.; Day, M.; Tao, Y.; Barrios, P.; Stupak, J.; Chan, K.; Li, J.; Chi, Y. *Adv. Funct. Mater.* **2007**, *17*, 1028. (m) Haeussler, M.; Liu, J.; Zheng, R.; Lam, W. Y.; Qin, A.; Tang, B. Z. *Macromolecules* **2007**, *40*, 1914.

(9) (a) Liu, C. H.; Chen, S. H.; Chen, Y. *J. Polym. Sci., A: Polym. Chem.* **2006**, *44*, 3882. (b) Lu, S.; Liu, T.; Ke, L.; Ma, D. G.; Chua, S. J.; Huang, W. *Macromolecules* **2005**, *38*, 8494. (c) Wu, C. W.; Tsai, C. M.; Lin, H. C. *Macromolecules* **2006**, *39*, 4298. (d) Liu, X. M.; Xu, J.; Lu, X.; He, C. *Macromolecules* **2006**, *39*, 1397. (e) Liu, C. L.; Chen, W. C. *Macromol. Chem. Phys.* **2005**, *206*, 2212. (f) Du, J.; Fang, Q.; Bu, D.; Ren, S.; Cao, A.; Chen, X. *Macromol. Rapid Commun.* **2005**, *26*, 1651.

(10) (a) Zhao, Z.; Zhao, Y.; Lu, P.; Tian, W. *J. Phys. Chem. C* **2007**, *111*, 6883. (b) Wu, C. W.; Lin, H. C. *Macromolecules* **2006**, *39*, 7232. (c) Li, M.; Tang, S.; Shen, F.; Liu, M.; Xie, W.; Xia, H.; Liu, L.; Tian, L.; Xie, Z.; Lu, P.; Hanif, M.; Lu, D.; Cheng, G.; Ma, Y. *J. Phys. Chem. B* **2006**, *110*, 17784. (d) Li, M.; Tang, S.; Shen, F.; Liu, M.; Xie, W.; Xia, H.; Liu, L.; Tian, L.; Xie, Z.; Lu, P.; Hanif, M.; Lu, D.; Cheng, G.; Ma, Y. *Chem. Commun.* **2006**, 3393. (e) Shih, P. I.; Chiang, C. L.; Dixit, A. K.; Chen, C. K.; Yuan, M. C.; Lee, R. Y.; Chen, C. T.; Diau, E. W. G.; Shu, C. F. *Org. Lett.* **2006**, *8*, 2799. (f) Wong, K. T.; Chen, Y. M.; Lin, Y. T.; Su, H. C.; Wu, C. C. *Org. Lett.* **2005**, *7*, 5361. (g) Ho, C.-L.; Wong, W.-Y.; Zhou, G.-J.; Yao, B.; Xie, Z.; Wang, L. *Adv. Funct. Mater.* **2007**, *17*, 2925.

(11) (a) Peng, Q.; Li, M.; Lu, S.; Tang, X. *Macromol. Rapid Commun.* **2007**, *28*, 785. (b) Promarak, V.; Ichikawa, M.; Sudyoadsuk, T.; Saengsuwan, S.; Jungsuttiwong, S.; Keawin, T. *Synth. Met.* **2007**, *157*, 17. (c) Bettington, S.; Tavasli, M.; Bryce, M. R.; Beeby, A.; Al-Attar, H.; Monkman, A. P. *Chem.—Eur. J.* **2007**, *13*, 1423. (d) Promarak, V.; Pankvuang, A.; Ruchirawat, S. *Tetrahedron Lett.* **2007**, *48*, 1151. (e) Grigalevicius, S.; Ma, L.; Xie, Z. Y.; Scherf, U. *J. Polym. Sci., A: Polym. Chem.* **2006**, *44*, 5987.

(12) (a) Powell, C. E.; Humphrey, M. G. *Coord. Chem. Rev.* **2004**, *248*, 725. (b) Abd-El-Aziz, A. S. *Macromol. Rapid Commun.* **2002**, *23*, 995. (c) Manners, I. *Science* **2001**, *294*, 1664. (d) Bunz, U. H. F. *Chem. Rev.* **2000**, *100*, 1605. (e) Zhang, N.; Hayer, A.; Köhler, A. *J. Chem. Phys.* **2006**, *124*, 244701.

(13) (a) Chen, J.; Chen, J.; Li, S.; Zhang, L.; Yang, G.; Li, Y. *J. Phys. Chem. B* **2006**, *110*, 4663. (b) Wasserberg, D.; Dudek, S. P.; Meskers, S. C. J.; Jansen, R. A. J. *Chem. Phys. Lett.* **2005**, *411*, 273.

(14) (a) Zelent, B.; Messier, P.; Gauthier, S.; Gravel, D.; Durocher, G. *J. Photochem. Photobiol., A: Chem.* **1990**, *52*, 165. (b) Zelent, B.; Messier, P.; Gravel, D.; Gauthier, S.; Durocher, G. *J. Photochem. Photobiol. A: Chem.* **1987**, *40*, 145. (c) Ganguly, T.; Sharma, D. K.; Gauthier, S.; Gravel, D.; Durocher, G. *J. Phys. Chem.* **1992**, *96*, 3757. (d) Brummer, K.; Dijken, A. V.; Börner, H.; Bastiaansen, J. J. A. M.; Kiggen, M. M.; Langeveld, B. M. W. *J. Am. Chem. Soc.* **2004**, *126*, 6035. (e) Cherkasov, Y.; Aleksandrova, E. L.; Piryatskii, Y. R. *Opt. Spektrosc.* **1999**, *87*, 943.

(15) Aly, S. M.; Ho, C.-L.; Fortin, D.; Wong, W.-Y.; Abd-El-Aziz, A. S.; Harvey, P. D. *Chem.—Eur. J.* **2008**, *14*, 8341.

(16) Blouin, N.; Leclerc, M. *Acc. Chem. Res.* **2008**, *41*, 1110.

(17) Chatt, J.; Shaw, B. L. *J. Chem. Soc.* **1960**, 4020.

(18) Kauffman, G. B.; Teter, L. A. *Inorg. Synth.* **1963**, *7*, 245.

(19) Wong, W. -Y.; Lu, G. -L.; Choi, K. -H.; Shi, J. -X. *Macromolecules* **2002**, *35*, 3506.

(20) Eaton, D. F. *Pure Appl. Chem.* **1988**, *60*, 1107.

(21) (a) Becke, A. D. *J. Chem. Phys.* **1993**, *98*, 5648. (b) Lee, C.; Yang, W.; Parr, R. G. *Phys. Rev. B: Condens. Matter Mater. Phys.* **1988**, 785.

(22) (a) Dobbs, K. D.; Hehre, W. J. *J. Comput. Chem.* **1986**, *7*, 359. (b) Dobbs, K. D.; Hehre, W. J. *J. Comput. Chem.* **1987**, *8*, 861.

(23) Anémian, R.; Mulatier, J. C.; Andraud, C.; Stéphan, O.; Vial, J. C. *Chem. Commun.* **2002**, 1608.

(24) Takahashi, S.; Kuroyama, Y.; Sonogashira, K.; Hagihara, N. *Synthesis* **1980**, 627.

(25) Khan, M. S.; Al-Mandhary, M. R. A.; Al-Suti, M. K.; Ahrens, B.; Mahon, M. F.; Male, L.; Raithby, P. R.; Boothby, C. E.; Köhler, A. *Dalton Trans.* **2003**, 74.

(26) Khan, M. S.; Al-Mandhary, M. R. A.; Al-Suti, M. K.; Hisahm, A. K.; Raithby, P. R.; Ahrens, B.; Mahon, M. F.; Male, L.; Marseglia, E. A.; Tedesco, E.; Friend, R. H.; Köhler, A.; Feeder, N.; Teat, S. J. *J. Chem. Soc., Dalton Trans.* **2002**, 1358.

(27) Liu, L.; Wong, W.-Y.; Shi, J.-X.; Cheah, K.-W.; Lee, T.-H.; Leung, L. M. *J. Organomet. Chem.* **2006**, *691*, 4028.
(28) McClure, D. S. *J. Chem. Phys.* **1949**, *17*, 905.
(29) Sonntag, M.; Strohriegl, P. *Chem. Mater.* **2004**, *16*, 4736.
(30) Zhang, L.-P.; Chen, B.; Wu, L.-Z.; Tung, C.-H.; Cao, H.; Tanimoto, Y. *Chem.—Eur. J.* **2003**, *9*, 2763.
(31) Faure, S.; Stern, C.; Espinosa, E.; Guilard, R.; Harvey, P. D. *Chem.—Eur. J.* **2005**, *11*, 3469.
(32) Harvey, P. D., *Recent Advances in Free and Metalated Multi-Porphyrin Assemblies and Arrays; A Photophysical Behavior and Energy Transfer Perspective*. In *The Porphyrin Handbook*; Kadish, K. M., Smith, K. M., Guilard, R., Eds.; Academic Press: San Diego, CA, 2003; Vol. *18*, p 63.
(33) Harvey, P. D.; Stern, C.; Gros, C.; Guilard, R. *J. Inorg. Biochem.* **2008**, *102*, 395.